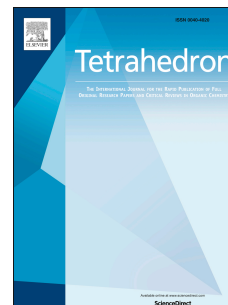


# Accepted Manuscript

Enhanced process development using automated continuous reactors by self-optimisation algorithms and statistical empirical modelling

Mohammed I. Jeraal, Nicholas Holmes, Geoffrey R. Akien, Richard A. Bourne



PII: S0040-4020(18)30221-7

DOI: [10.1016/j.tet.2018.02.061](https://doi.org/10.1016/j.tet.2018.02.061)

Reference: TET 29332

To appear in: *Tetrahedron*

Received Date: 23 October 2017

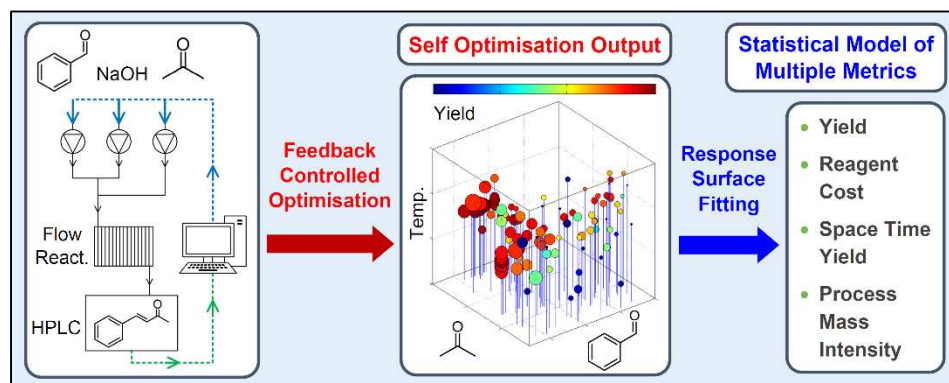
Revised Date: 22 February 2018

Accepted Date: 24 February 2018

Please cite this article as: Jeraal MI, Holmes N, Akien GR, Bourne RA, Enhanced process development using automated continuous reactors by self-optimisation algorithms and statistical empirical modelling, *Tetrahedron* (2018), doi: 10.1016/j.tet.2018.02.061.

This is a PDF file of an unedited manuscript that has been accepted for publication. As a service to our customers we are providing this early version of the manuscript. The manuscript will undergo copyediting, typesetting, and review of the resulting proof before it is published in its final form. Please note that during the production process errors may be discovered which could affect the content, and all legal disclaimers that apply to the journal pertain.

## Graphical Abstract



## Enhanced process development using automated continuous reactors by self-optimisation algorithms and statistical empirical modelling

Mohammed I. Jeraal,<sup>1</sup> Nicholas Holmes,<sup>1</sup> Geoffrey R. Akien<sup>1,2</sup> and Richard A. Bourne\*<sup>1</sup>

Address: <sup>1</sup>Institute of Process Research and Development, School of Chemistry & School of Chemical and Process Engineering, University of Leeds, Leeds, LS2 9JT, UK; and <sup>2</sup>Department of Chemistry, Faraday Building, Lancaster University, Lancaster, LA1 4YB, UK

\* Corresponding author

Email: Richard A. Bourne – [R.A.Bourne@leeds.ac.uk](mailto:R.A.Bourne@leeds.ac.uk)

## Abstract

Reaction optimisation and understanding is fundamental for process development and is achieved using a variety of techniques. This paper explores the use of self-optimisation and

experimental design as a tandem approach to reaction optimisation. A Claisen-Schmidt condensation was optimised using a branch and fit minimising algorithm, with the resulting data being used to fit a response surface model. The model was then applied to find new responses for different metrics, highlighting the most important for process development purposes.

## Keywords

self-optimisation; design of experiments; Claisen-Schmidt condensation; reaction metrics; process development, flow chemistry

## Introduction

Traditional univariate optimisation of a chemical reaction involves the systematic and sequential optimisation of each individual reaction parameter until an optimum is found. While the execution is simple, the data will not account for interactions between reaction parameters.<sup>1</sup> Design of experiments (DoE) conversely uses statistical calculations to screen reactions and generate a polynomial model over a constrained area of experimental space. The model can highlight the key parameters and interactions that affect changes in the desired response, as well as predicting new responses depending on the model's design. The methodology is commonly utilised in the pharmaceutical industry, particularly for reactions with poor yield, inconsistent output or unexpected results upon scale up.<sup>2</sup> DoE is a very powerful tool and it can show where improvements in operating conditions can be made to deliver a more consistent and reliable product with respect to the optimisation target.

One of the disadvantages of DoE arises when there are a large number of parameters requiring optimisation. The number of experiments required for a design increases substantially with an

increasing number of experimental parameters. Often this number can be too large to explore the system efficiently, so a fractional factorial design is implemented to reduce the number of experiments. The disadvantage with this approach is that at least one parameter is confounded with an interaction, thus increasing the complexity of the model analysis. It is also very important that the correct limits are chosen for each parameter to ensure that there are no sudden changes in response and a good polynomial fit can be achieved. Furthermore, additional experiments might be required to verify a response, deconvolute interactions or determine the robustness of optimum conditions.

Self-optimisation is a technique that could remove the problems associated with DoE whilst still obtaining the important information about key parameters and interactions. A self-optimising reactor combines on-line analysis with an adaptive feedback loop and minimizing algorithm to autonomously execute reactions, obtain the respective yields and ultimately optimise a chemical process without user intervention.<sup>3-8</sup> The algorithm typically generates a cluster of points around an optimum, therefore increasing the robustness of proposed optimal conditions.

The recent popularity of self-optimisation is increasing but its use in industrial chemical processes is severely limited.<sup>9</sup> A continuous self-optimising reactor will benefit from the numerous advantages of flow reactors including high surface area to volume ratios, safer operation of hazardous materials, improved mixing, faster kinetics and easier access to automated processes.<sup>10-13</sup>

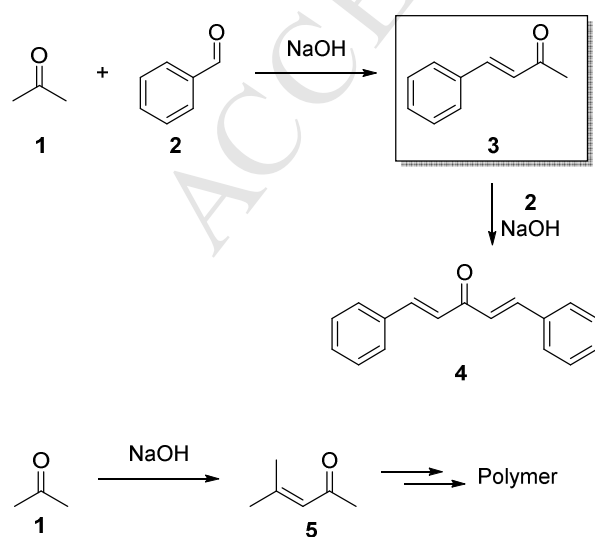
The main disadvantage with self-optimisation is that new experiments need to be physically executed to optimise for a new target or different chemical compound. If DoE has already been carried out, new models for different responses can be calculated without complication or increased experimentation.

This paper attempts to combine these two optimisation techniques in parallel. A self-optimisation experiment will rapidly generate optimum conditions and scatter across the

chemical space through an exploratory algorithm, whilst a response surface model (RSM) will permit the prediction of new responses using the experimental data.

## Results and Discussion

Self-optimising reactors have been designed using a variety of analytical techniques including IR<sup>14-16</sup> and NMR spectroscopy<sup>17</sup>, mass spectrometry<sup>16,18</sup>, gas<sup>19-22</sup> and liquid<sup>23,24</sup> chromatography. In this paper, a feedback-controlled flow reactor, equipped with an at-line HPLC system, is used to provide fast separation and quantification of the desired compounds. Through the combined implementation of a variable wavelength UV detector and microvolume sample injector, automated optimisations were executed at the mesoscale with the direct injection of reaction mixture into the HPLC column, thus negating the need for dilution prior to analysis. The optimisation target was the minor product of a Claisen-Schmidt condensation between acetone (**1**) and benzaldehyde (**2**) to form the desired product, benzylideneacetone (**3**) (Scheme 1).<sup>25</sup> Strict control over the reaction parameters was required to prevent **3** reacting to form dibenzylideneacetone (DBA) (**4**) and acetone polymerization, both of which caused clogging in the reactor.



**Scheme 1:** Claisen-Schmidt condensation between acetone (**1**) and benzaldehyde (**2**) to form the desired benzylideneacetone (**3**) and undesired benzylideneacetone (**4**). Acetone can also undergo self-condensation to form mesityl oxide (**5**), as well as the subsequent polymer.

A gradient HPLC method at 254 nm was developed to quantify compounds of interest. While adequate separation between species was achieved, preliminary HPLC calibrations resulted in a non-linear response for **2** and **3** at the reference wavelength of 254 nm. UV spectra of both compounds were obtained to determine the wavelengths at which each species could be quantified, without saturating the detector (Figure 1). The HPLC method was consequently modified to momentarily switch to 295 nm and 333 nm, when compounds **2** and **3** were respectively eluted, to ensure the detector would not be saturated during optimisation. This new method allowed linear calibrations of species **2-5**.

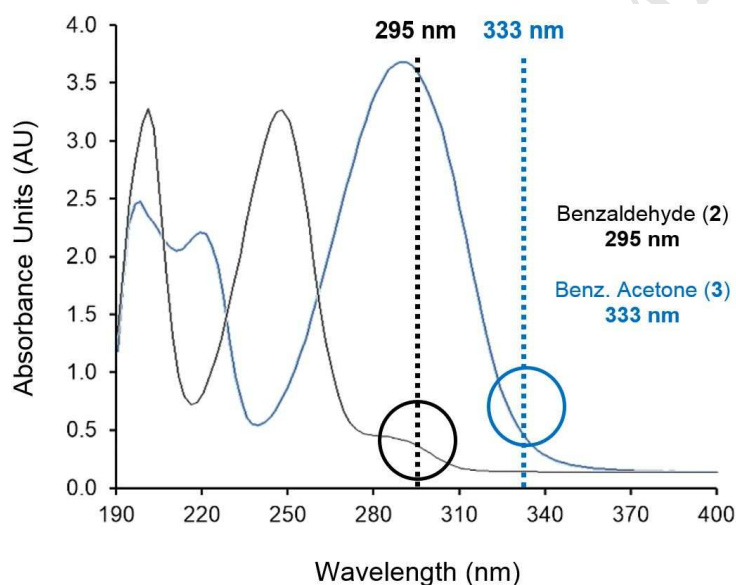


**Figure 1:** UV absorption spectra of benzaldehyde (**2**) and benzylideneacetone (**3**) in ethanol between 190 and 400 nm. Dashed lines indicate wavelengths selected for variable wavelength HPLC method.

All components were monitored and controlled via a bespoke MATLAB based software package (Reaction setup is shown Figure 6). The flow rates of the three reagent pumps and reactor temperature were varied to maximise the yield of **3**. Table 1 displays the optimisation limits for the four reaction variables. Acetone flow was controlled relative to **2** to ensure it was always in excess, while the temperature was limited to 80°C after initial experiments exhibited polymer formation beyond this. While previous literature and preliminary experiments can be used to constrain the experimental space and speed up the optimisation process, the algorithm is also capable of optimising within the entire operating range of the equipment being utilised. This capability is particularly advantageous when no prior knowledge of a chemical process is available.

The algorithm used for the optimisation was SNOBFIT, a constrained branch and fit function that locates optima by fitting polynomials to the response of experimental data points.<sup>26</sup> During an optimisation it focuses on locating optimal conditions, whilst simultaneously exploring empty space to prevent premature termination at local optima. In the event of multiple optima within a chemical system, the algorithm is capable of exploring both regions of experimental space within a single experiment.

**Table 1:** Parameter limits for the automated optimisation to maximise yield of **3**

Reaction Variable	Benzaldehyde <b>2</b> Flow / mmol min <sup>-1</sup> <sup>a</sup>	NaOH Flow / mmol min <sup>-1</sup> <sup>b</sup>	Acetone Flow / mol. equivalent. <sup>c</sup>	Temperature / °C
Limits	0.4 – 2.0	0.04 – 0.25	1 – 7	10 – 80

<sup>a</sup>1.95 M solution in ethanol with 0.0325 M biphenyl internal standard; <sup>b</sup>0.2 M solution in ethanol; <sup>c</sup>neat liquid, controlled with respect to flow rate of **2**

The optimisation cycle was repeated until a total of 70 experiments had been executed. The results (Figure 2) indicate that an optimum yield of 66.0% was achieved at a benzaldehyde (**2**) flow rate of 0.4 mmol/min, with 7 molar equivalents of acetone and a reactor temperature of 35.8 °C. The catalyst concentration of 0.25 M is also displayed in molar equivalents relative to benzaldehyde to ease comparability between runs. Because the catalyst concentration was regulated in mmol/min (Table 1), the algorithm minimised the flow rate of benzaldehyde to 0.4 mmol/min, whilst maximising the catalyst flow rate to 0.25 mmol/min, to achieve this maximum equivalence. While the cluster of high yield experiments surrounding the optimum were all executed at maximum NaOH equivalence, there are other experiments exhibiting yields of around 60%, with much lower NaOH equivalents, which suggests that catalyst concentration may not be the most significant yield limiting factor in this reaction. Following the data points along the y-axis suggests there is some dependence on acetone concentration. This is better appreciated when the data is viewed along the y-axis (Figure 2b) where this is a clear correlation between acetone equivalence and yield.

There is an interaction between the benzaldehyde and NaOH flow rates and temperature, which can be observed through the points at maximum acetone equivalence. As the flow rate of benzaldehyde (**2**) increases, NaOH decreases in order to accommodate for the decrease in residence time. This is paired with an increase in temperature to achieve higher yields at lower catalyst loadings. This all contributes to a large area of points resembling a cliff edge at the border of the experimental space.

As predicted, formation of DBA (**4**) increases at lower acetone concentrations with a maximum yield occurring at 3.1 molar equivalences. Below this concentration, formation of ketone **3** may be hindered by a reduced rate of acetone enolate formation.<sup>27</sup>

The residence time was calculated for each set of conditions to determine the point at which the sample eluting from reactor, was representative of the preset experimental parameters. Most experiments exhibited a residence time between 5 and 15 mins. Given that multiple



experiments across this range exhibited yields in excess of 60%, residence time was not deemed to have a significant impact on the yield of **3**. However, for chemical processes where a given optimisation target is dependent on residence time, the system autonomously optimises this parameter within the confines of the flow rate limits.

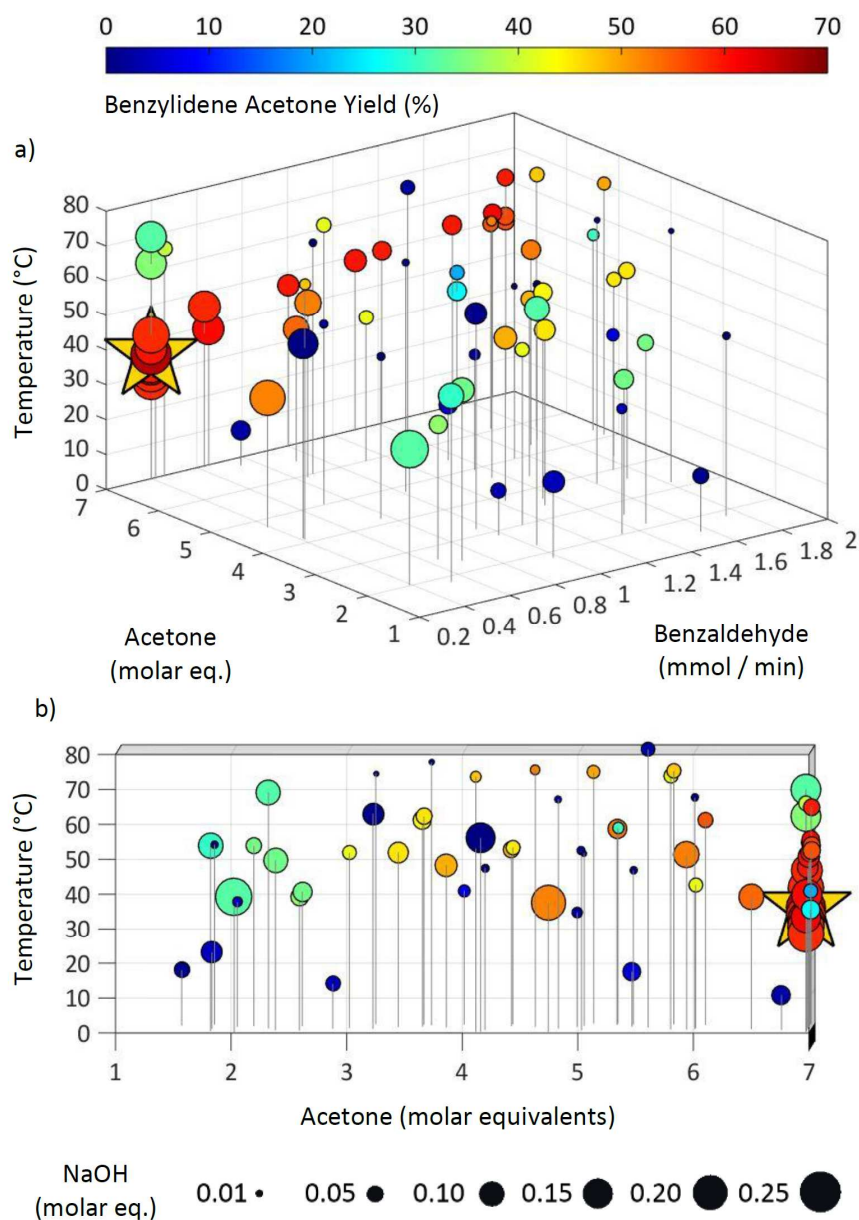


**Figure 2:** a): Each point represents one of the experiments executed during the optimisation. Graph displays five variables as follows: (x) molar flow rate of benzaldehyde, (y) molar equivalents of acetone, (z) temperature of tubular flow reactor. The point size denotes the

NaOH catalyst concentration in each run. The colour of each point represents the yield (%) of **3** in relation to **2**. A maximum yield of 66.0% was achieved, the conditions of which are highlighted by the star. b) Identical to a) but rotated to depict data as viewed along the y-axis.

The formation of other UV active species which were not calibrated prior to the optimisation could also be monitored because a full HPLC chromatogram was collected for each set of reaction conditions. Any compounds of interest could be characterised against reference materials and subsequently quantified following a HPLC calibration. The HPLC method switches to 254 nm outside regions of interest to maximise absorption resulting from ancillary organic species. This, coupled with the direct injection of sample into the instrument, ensures that even low level products can be detected.

The concentration of any compound can later be increased with the corresponding yield optimisation.<sup>22</sup> The existing responses can be used as a starting point to limit the number of experiments required for completion, but additional optimisations ultimately result in an increase of time and resource. A better methodology could be to predict where unknown compounds have the highest yields and then carry out yield optimisations in a smaller operating window around that point. This can be achieved by fitting a response surface to the existing data.

Response surfaces were obtained for compounds **2**, **3** and **4** using a multiple linear regression (MLR) fit.<sup>28</sup> Models were first generated by including all square and interaction terms, then removing non-significant coefficients for which the calculated error potentially equalled zero. Next, experiments were removed that fell beyond  $\pm 2.5$  standard deviations (SD) on a normal probability residual plot. Outliers are typically removed (or repeated) if they fall outside of  $\pm 4$  SD but the lower tolerance in this instance allowed for a better fit and greater predictability. The lowest number of experiments in a model was 65, which was in excess of the requirement for a central composite design, which is 24 plus mid-points. The prior removal of high error

experiments was therefore not deemed to numerically compromise the model. A good fit was achieved for all three compounds with  $R^2$  values of 0.73 (**2**), 0.91 (**3**) and 0.85 (**4**). These models also showed a moderate level of predictability with  $Q^2$  values of 0.66 (**2**), 0.86 (**3**) and 0.78 (**4**).

The models were subsequently used to predict an optimum yield by maximising the response of **3** (minimum tolerance 65%) and minimising **2** and **4** (maximum tolerance 5%). Conditions obtained that satisfied two of those criteria were: 1.97 mol/min of **2**, 4.8 molar eq. of acetone, 0.1 mmol/min of NaOH and a reactor temperature of 80 °C, generating **3** in a 61.1% yield. These conditions do not match the optimal conditions generated by the self-optimisation, for which the model calculates a yield of 59.5 %. Both the predicted and experimental optima are within the error associated with HPLC analysis, indicating that there is a plateau of conditions that generate **3** at approximately 60% yield.

Further scrutiny of the SNOBFIT optimum data point showed that there was a significant rise in yield compared to points in close vicinity. This, coupled with the disagreement in optima between the two techniques prompted some further experimentation to study the reproducibility of the algorithm optimum. Three further experiments were carried out at the optimum conditions, which generated **3** in a mean yield of 64.4%  $\pm$  0.3% (arithmetic mean  $\pm$  1 SD). This shows that the previous optimum value was possibly caused by an integration error from HPLC analysis.

A second self-optimisation for the generation of **3** was executed to determine if yields could be further increased by expanding on the existing experimental space. As lower acetone equivalents previously displayed lower yields, Table 2 shows how acetone equivalence limits were increased from 1-7 to 5-14 molar equivalents. The maximum NaOH flow rate was also increased to 0.1 mmol/min as the optimum point was at its upper limit. Whilst the model-predicted optimum was close to the maximum upper limit of benzaldehyde flow rate, this

parameter limit was halved (to 1 mmol/min) to compensate for the increase in experimental space and minimise the detriment to operating efficiency. The maximum temperature was also reduced from 80 to 60 °C for the same reasons.

The SNOBFIT algorithm was then restarted using existing data within the new operating conditions (Table 2). The new optimisation required 36 further experiments and produced optimum conditions of 0.76 mmol/min of **2**, 14 eq of acetone, 0.15 mmol/min of NaOH, and a temperature of 43 °C, generating **3** in a 67% yield (Figure 3).

**Table 2.** Parameter limits for the extended optimisation to maximise yield of **3**.

Reaction Variable	Benzaldehyde <b>2</b> Flow / mmol min <sup>-1</sup> <sup>a</sup>	NaOH Flow / mmol min <sup>-1</sup> <sup>b</sup>	Acetone Flow / mol. equivalent. <sup>c</sup>	Temperature / °C
Limits	0.4 – 1.0	0.10 – 0.25	5 – 14	10 – 60 °C

<sup>a</sup>1.95 M solution in ethanol with 0.0325 M biphenyl internal standard; <sup>b</sup>0.2 M solution in ethanol; <sup>c</sup>neat liquid, regulated with respect to flow rate of **2**

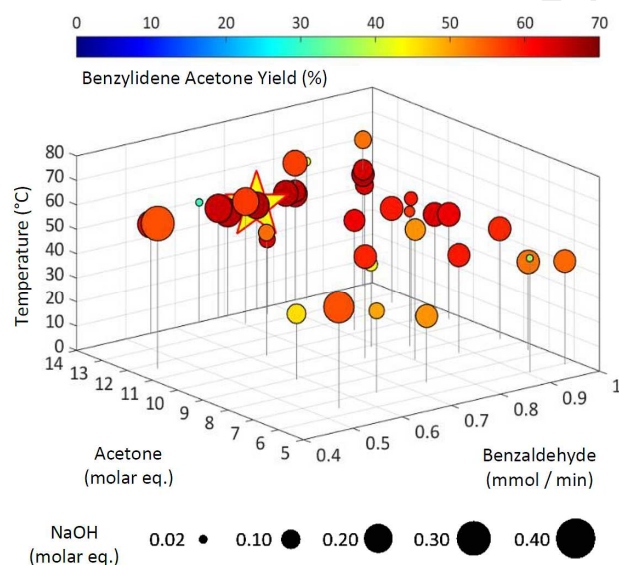


**Figure 3.** Plot of experiments performed during extended automated yield optimisation of benzylideneacetone (**3**) via the aldol condensation of benzaldehyde (**2**) with acetone. The graphical parameters are identical to Figure 2, while the optimisation parameters have both

been adjusted to allow for more acetone and catalyst equivalents versus the first yield optimisation (see Table 2). A maximum yield of 66.6% was achieved as highlighted by the star.

New models were fitted using the same approach and improved  $R^2$  (fit) and  $Q^2$  (predictability) was achieved for all models using the data from the extended optimisation (Figure 4 **Error! Reference source not found.**). Optimum conditions were predicted as previously described and the model calculated revised conditions to generate product **3** in a 63.6 % yield (Figure 5). Whilst this yield is still lower than the experimental self-optimisation, the expansion of experimental space has resulted in an increased yield from the previously predicted result of 61.1%. The conditions also correlate better with the optimum produced by self-optimisation (0.741 mmol/min of **2**, 12.4 mol. eq of **1**, 0.112 mmol/min of NaOH at 47.2 °C).

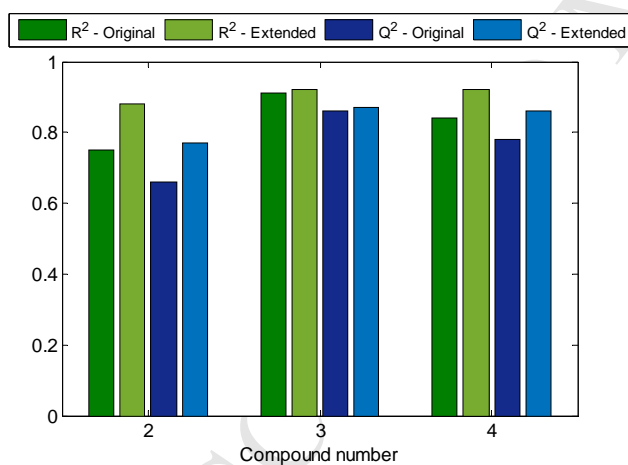


**Figure 4.** Comparison of the change in  $R^2$  and  $Q^2$  between the models generated from the original and extended data.

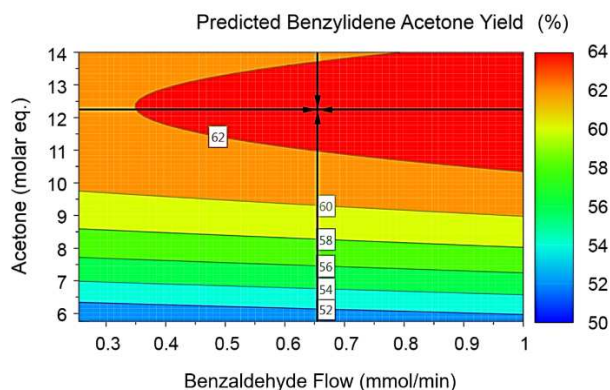


**Figure 5:** Contour plot of predicted benzylideneacetone yields using original and extended data. Optimum point with a predicted yield of 63.6% is shown by crosshair.

While it seems achievable to improve the maximum observed product **3** yield of 67% by extending the experimental space to allow for greater acetone and hydroxide equivalents, it is worth considering whether increasing the reagent cost in pursuit of a higher product yield would be financially or materially efficient upon scale up of the reaction. Although yield was the target parameter in this optimisation, previous research has demonstrated how these systems can be utilised to optimise other metrics such as E factor, process mass intensity and reaction productivity to improve the sustainability of a chemical process.<sup>16,23,29,30</sup> The advantage of a statistical model following self-optimisation means that such metric analyses can be carried out without further practical experiments.

This ability to predict alternative metrics has been demonstrated by further fitting of the experimental data used to create the existing models. The metrics explored in this study were process mass intensity (PMI),<sup>31</sup> a measure of the total chemical resource per mass unit of product; space time yield (STY), the mass of product formed per unit volume per unit time; and the raw material cost per kg of product (see supporting information for calculations). New

models for these metrics were fitted using MLR with  $R^2$  values of 0.93 (PMI), 0.92 (STY) and 0.90 (cost); and  $Q^2$  values of 0.86 (PMI), 0.86 (STY) and 0.83 (cost).

**Table 3.** Effect of different metrics on the product composition of compounds **2-4**

Metric target	<b>2</b> / % Yield	<b>3</b> / % Yield	<b>4</b> / % Yield	PMI	STY / g L <sup>-1</sup> h <sup>-1</sup>	Cost / £ kg <sup>-1</sup>
Yield	3.22	<b>65.62</b>	<i>3.01</i>	18.48	633.20	33.45
PMI	4.54	47.90	6.02	<i>13.81</i>	614.36	27.92
STY	3.06	62.15	4.45	19.11	<b>872.69</b>	34.50
Cost	4.15	58.81	4.13	14.30	798.39	26.72
Yield PMI <sup>a</sup>	4.28	<b>55.32</b>	<i>4.70</i>	<i>13.99</i>	729.52	26.91
PMI Cost <sup>b</sup>	2.96	64.81	3.66	<i>16.35</i>	769.93	29.57

The first column shows the metric target, responses are shown in the rows. Maximum values are highlighted in bold, minimized values are highlighted in italics. Unformatted values display the models' predicted values. <sup>a</sup>maximise the yield of **3** whilst minimising the PMI; <sup>b</sup>minimise both PMI and cost.

Table 3 shows how the model responses change with optimum conditions for different metric targets. The maximum yield exhibits poor responses for PMI, STY and cost, showing how high yielding reactions can be wasteful and unproductive. The optimum response for PMI is the least productive and for the studied metrics, predicts the lowest yield for **3** at 48%. There is good correlation between the responses of PMI and cost for all the metric targets. This should be expected as both are dependent on the ratio of product to substrates and reagents. The raw material cost calculation aims to put bias on reducing the concentrations of expensive material. However, this reaction may not best represent this capability as all substrates are relatively inexpensive. It should be noted that lower cost promotes a higher yield to a greater

extent than lower PMI, thus indicating that raw material cost could be the most important metric in this reaction format. This is assuming that the adoption of cheaper reagent does not increase the reaction complexity and therefore increase the cost of work-up and purification.

**Table 4.** Predicted conditions for the optimum responses to different metric targets

Metric target	<b>2</b> Flow / mmol min <sup>-1</sup>	NaOH Flow / mmol min <sup>-1</sup>	Acetone / equivalents	Temperature / °C
Yield	0.741	0.112	12.4	47.2
PMI	0.846	0.044	6.0	44.1
STY	1.000	0.150	13.9	42.2
Cost	0.986	0.067	9.2	47.1
Yield PMI <sup>a</sup>	0.915	0.055	7.5	45.5
PMI Cost <sup>a</sup>	0.998	0.096	10.5	46.8

<sup>a</sup>maximize the yield of **3**, minimize the PMI; <sup>b</sup> minimize both PMI and cost.

The conditions for the optimal responses are shown in Table 4. The flow rate of **2** is close to its upper limit for every target. This reduces the residence time and consequently increases the reaction productivity (STY). The acetone equivalents are generally lower than those generated by the yield driven self-optimisation, thus limiting the reagent waste (through PMI and cost). Strict temperature control is required in compensation to maintain the high yields of **3**, whilst minimising risk of polymer formation.

## Conclusion

The yield of a minor product in a Claisen-Schmidt condensation has been optimised using a self-optimising flow reactor equipped with an online HPLC system. The reaction in this paper



was optimised directly at the mesoscale to produce 0.24 kg/day of the desired benzylideneacetone, **3**. Through the development of a variable wavelength HPLC method, all organic species of interest could be quantified within their respective linear detection limits.

With the data obtained from the self-optimisation, a response surface was fitted to the main compounds of interest in the reaction (**2-4**). After an analysis of the self-optimisation data and resulting models, it was decided to execute a further optimisation in a larger chemical space. The second experimental optimisation improved upon the yield of **3** and the increased correlation between the new optimum and surrounding experimental points, provided a greater range of conditions at which optimal yields could be obtained. The subsequent statistical model of the extended optimisation also predicted similar optimal conditions.

It should be noted that the choice of algorithm in the initial self-optimisation step is critical to achieving a good fit to the RSM. The simplex algorithm and modifications thereof,<sup>32-35</sup> are a popular choice in self-optimising systems.<sup>16,17,19-24</sup> During operation, however, only experiments with an improved predicted response will be executed, therefore negating valuable information existing in the experimental space between the initial and optimum points. The execution of random conditions and exploration of free space offered by SNOBFIT provides a scatter of data, without which the additional response surface fitting would not be possible. In this study, the increased robustness resulting from the additional experimental points around the optimum would also have been forfeited with a simplex approach.

In this example, the experimental optimum was identified at the edge of the initial optimisation space. Prediction of the optimum via the statistical model was therefore compromised due to the inability to fit a polynomial to changes induced by the cliff edge. The experimental self-optimisation, however, freely explored the edge of the optimisation space to identify the point of maximum yield. For these reasons, we believe that self-optimisation is

the superior technique for chemical process optimisation. When used in tandem, however, the subsequent response fitting of self-optimisation data can predict the responses of different species and even alternate metrics without additional experimentation. It therefore follows that self-optimisation and DoE can be interdependent, rather than conflicting techniques, which can combine to provide a wealth of information in the scale-up and process optimisation of chemical systems.

## Experimental

**Automated yield optimisation:** Reaction control, yield calculation and process optimisation were under full MATLAB automation via a bespoke program utilising the SNOBFIT optimisation algorithm. The reactor was setup as displayed in Figure 6 for HPLC calibration and experimental yield optimisations.

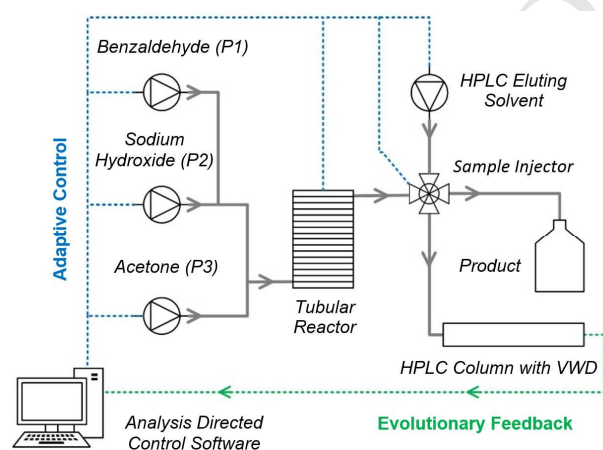


**Figure 6:** Schematic of automated self-optimising flow reactor. Bespoke MATLAB based control software monitored and regulated the following: flow rate and pressure of the reagent pumps (P1, P2 & P3); temperature of the tubular reactor and activation of the sample injector. Reagents were pumped at the specified flow rates through individual Jasco PU-980 HPLC pumps and mixed via Swagelock 1/16" tee-pieces. The reaction mixture was heated to the

specified temperature using a Polar Bear Plus Flow Synthesizer. A sample from each set of conditions was acquired by a VICI Valco 4 Port Microvolume Sample Injector. HPLC analysis was carried out by an Agilent 1100 HPLC System with G1314B Variable Wavelength Detector. Pressure was maintained using a Jasco BP-1580 Back Pressure Regulator and Polyflon 1/16" (OD) PTFE tubing was utilised throughout the 6.5 ml reactor.

Five sets of reaction conditions were initially selected and autonomously executed by the software. The yields of these experiments were calculated from the HPLC response using a biphenyl present in the reagent. Subsequent conditions were then generated by fitting yield responses to the data using the SNOBFIT. 70 experiments were executed as 14 cycles of 5 experiments under full MATLAB automation. Following initial response fitting, an additional 36 experiments were carried as described in Table 2.

**Variable wavelength HPLC Method:** Calibration and optimisation analyses were executed using an Agilent 1100 Series HPLC System equipped with a G1312A binary pump and G1314B variable wavelength detector (VWD). Compounds were separated via an Ascentis Express C18 column (5.0  $\mu\text{m}$  particle size, 4.6 mm diameter x 50 mm length). Mobile phase was a binary mixture of acetonitrile and water (MeCN-H<sub>2</sub>O), each containing 0.1% (v/v) of trifluoroacetic acid. Method was gradient based with a 5:95 (v/v) MeCN-H<sub>2</sub>O starting mixture. Concentration was immediately increased to 95:5 (v/v) MeCN-H<sub>2</sub>O via a 7 min linear gradient, followed by an immediate decrease back to 5:95 (v/v) MeCN-H<sub>2</sub>O via a 2 min linear gradient, where it remained for 1 min. Total run time was 10 mins at a constant flow rate of 1.2 ml/min with a column temperature of 20 °C throughout. The absorption wavelength of the VWD operates at base value of 254 nm. 3.4 mins into the method, the wavelength switches to 295 nm for 0.2 mins. At 4.2 mins, there is a switch to 333 nm for 0.2 mins.

**Acquisition of UV spectra:** 2 M solutions of **2** and **3** in ethanol were manually injected through an Agilent 1100 HPLC System with G1314B variable wavelength detector. A UV absorption spectrum between 190 and 400 nm was captured for each species upon elution.

**HPLC Calibration:** Reactor was setup as depicted in Figure 6. A solution of analyte (2.0 M) was pumped against solvent at varying flow rates, with a total flow of 1 ml/min, to create a 10-point calibration graph. Two reactor volumes of material was eluted prior to HPLC sample injection. Flow rates and sample injection were autonomously controlled via a MATLAB based program.

**Statistical Modelling:** Multiple linear regression fits were applied to the automated experimental results using the MODDE software package from UMetrics. Predicted responses for the yields of compounds **2**, **3** and **4**, as well as reaction metrics including process mass intensity, space time yield, and bulk cost of reagents were obtained using multiple linear regression. Interactions with the potential of zero contribution to the measured response, as well as individual experiments with high residual error were negated to maximise the model fitting.

See ESI for full details on the reactor setup, HPLC method, individual parameters for the automated yield optimisations and the statistical analysis methodology.

## Acknowledgements

The authors would like to thank Rebecca Meadows, Robert Woodward and Brian Taylor from AstraZeneca for project support, Matthew Broadbent for workshop support and Simon Barrett and Martin Huscroft for analytical support as well as Bao Nguyen and group. NH thanks EPSRC, AstraZeneca and University of Leeds for a DTG case funded studentship.

## References

1. Rasheed, M.; Wirth, T. *Angew. Chem., Int. Ed.* **2011**, *50*, 357-358.
2. Weissman, S. A.; Anderson, N. G. *Org. Process Res. Dev.* **2015**, *19*, 1605-1633.
3. Krishnadasan, S.; Brown, R. J. C.; deMello, A. J.; deMello, J. C. *Lab on a Chip* **2007**, *7*, 1434-1441.
4. McMullen, J. P.; Stone, M. T.; Buchwald, S. L.; Jensen, K. F. *Angewandte Chemie International Edition* **2010**, *49*, 7076-80.
5. Skilton, R. A.; Bourne, R. A.; Amara, Z.; Horvath, R.; Jin, J.; Scully, M. J.; Streng, E.; Tang, S. L. Y.; Summers, P. A.; Wang, J.; Perez, E.; Asfaw, N.; Aydos, G. L. P.; Dupont, J.; Comak, G.; George, M. W.; Poliakoff, M. *Nature Chemistry* **2015**, *7*, 1-5.
6. Fabry, D. C.; Sugiono, E.; Rueping, M. *React. Chem. Eng.* **2016**.
7. Holmes, N.; Bourne, R. A. In *Chemical Process Technology for a Sustainable Future*; Letcher, T. M.; Scott, J. L.; Paterson, D. A. Eds.; RSC Publishing, 2014; pp. 28-45.
8. Sans, V.; Cronin, L. *Chem. Soc. Rev.* **2016**, *45*, 2032-2043.
9. Holmes, N.; Akien, G. R.; Blacker, A. J.; Woodward, R. L.; Meadows, R. E.; Bourne, R. A. *React. Chem. Eng.* **2016**, *1*, 366-371.
10. Hessel, V. *Chem. Eng. Technol.* **2009**, *32*, 1655-1681.
11. Wegner, J.; Ceylan, S.; Kirschning, A. *Adv. Synth. Catal.* **2012**, *354*, 17-57.
12. Ley, S. V.; Fitzpatrick, D. E.; Ingham, R. J.; Myers, R. M. *Angew. Chem. Int. Ed.* **2015**, *54*, 3449-3464.
13. Ley, S. V.; Fitzpatrick, D. E.; Myers, R. M.; Battilocchio, C.; Ingham, R. J. *Angew. Chem., Int. Ed.* **2015**, *54*, 10122-10136.
14. Skilton, R. A.; Parrott, A. J.; George, M. W.; Poliakoff, M.; Bourne, R. A. *Appl. Spectrosc.* **2013**, *67*, 1127-1131.
15. Mattrey, F.; Dolman, S.; Nyrop, J.; Skrdla, J. *Am. Pharm. Rev.* **2012**, *15*.
16. Fitzpatrick, D. E.; Battilocchio, C.; Ley, S. V. *Org. Process Res. Dev.* **2015**, *20*, 386-394.
17. Sans, V.; Porwol, L.; Dragone, V.; Cronin, L. *Chem. Sci.* **2015**, *6*, 1258-1264.
18. Holmes, N.; Akien, G. R.; Savage, R. J. D.; Stanetty, C.; Baxendale, I. R.; Blacker, A. J.; Taylor, B. A.; Woodward, R. L.; Meadows, R. E.; Bourne, R. A. *React. Chem. Eng.* **2016**, *1*, 96-100.
19. Parrott, A. J.; Bourne, R. A.; Akien, G. R.; Irvine, D. J.; Poliakoff, M. *Angew. Chem., Int. Ed.* **2011**, *50*, 3788-3792.
20. Bourne, R. A.; Skilton, R. A.; Parrott, A. J.; Irvine, D. J.; Poliakoff, M. *Org. Process Res. Dev.* **2011**, *15*, 932-938.
21. Jumbam, D. N.; Skilton, R. A.; Parrott, A. J.; Bourne, R. A.; Poliakoff, M. *J. Flow Chem.* **2012**, *2*, 24-27.
22. Amara, Z.; Streng, E. S.; Skilton, R. A.; Jin, J.; George, M. W.; Poliakoff, M. *Eur. J. Org. Chem.* **2015**, *2015*, 6141-6145.
23. McMullen, J. P.; Jensen, K. F. *Org. Process Res. Dev.* **2010**, *14*, 1169-1176.
24. McMullen, J. P.; Stone, M. T.; Buchwald, S. L.; Jensen, K. F. *Angew. Chem., Int. Ed.* **2010**, *49*, 7076-7080.
25. Drake, N. L.; Allen, P. *Org. Synth.* **1923**, *3*, 17-20.
26. Huyer, W.; Neumaier, A. *ACM Trans. Math. Softw.* **2008**, *35*, 1-25.
27. Tanaka, K.; Motomatsu, S.; Koyama, K.; Fukase, K. *Tetrahedron Lett.* **2008**, *49*, 2010-2012.
28. Umetrics MODDE; Sartorius Stedim Biotech.
29. Jumbam, D. N.; Skilton, R. A.; Parrott, A. J.; Bourne, R. A.; Poliakoff, M. *Journal of Flow Chemistry* **2012**, *2*, 24-27.
30. Skilton, R. A.; Parrott, A. J.; George, M. W.; Poliakoff, M.; Bourne, R. A. *Applied Spectroscopy* **2013**, *67*, 1127-31.
31. Jimenez-Gonzalez, C.; Ponder, C. S.; Broxterman, Q. B.; Manley, J. B. *Org. Process Res. Dev.* **2011**, *15*, 912-917.
32. Spendley, W.; Hext, G. R.; Himsforth, F. R. *Technometrics* **1962**, *4*, 441-461.
33. Nelder, J. A.; Mead, R. *Comput. J.* **1965**, *7*, 308-313.
34. Routh, M. W.; Swartz, P. A.; Denton, M. B. *Anal. Chem.* **1977**, *49*, 1422-8.
35. Kazmierczak, R. F. *Optimizing Complex Bioeconomic Simulations Using An Efficient Search Heuristic*; DAE Research Report, 1996.